

Solar radiation management and ecosystem functional responses

Akihiko Ito^{1,2} 

Received: 30 September 2016 / Accepted: 10 February 2017 / Published online: 2 March 2017
© Springer Science+Business Media Dordrecht 2017

Abstract Geoengineering such as solar radiation management (SRM) can be an emergent option to avoid devastating climatic warming, but its ramifications are barely understood. The perturbation of the Earth's energy balance, atmospheric dynamics, and hydrological cycling may exert unexpected influences on natural and human systems. In this study, I evaluate the impacts of SRM deployment on terrestrial ecosystem functions using a process-based ecosystem model (the Vegetation Integrative Simulator for Trace gases, VISIT) driven by the climate projections by multiple climate models. In the SRM-oriented climate projections, massive injection of sulphate aerosols into the stratosphere lead to increased scattering of solar radiation and delayed anthropogenic climate warming. The VISIT simulations show that canopy light absorption and gross primary production are enhanced in subtropics in spite of the slight decrease of total incident solar radiation. The retarded temperature rise during the deployment period leads to lower respiration, and consequently, an additional net terrestrial ecosystem carbon uptake by about 20%. After the SRM termination, however, along with the temperature rise, this carbon is released rapidly to the atmosphere. As a result of altered precipitation and radiation budget, simulated runoff discharge is suppressed mainly in the tropics. These SRM-induced influences on terrestrial ecosystems occur heterogeneously over the land surface and differed among the ecosystem functions. These responses of terrestrial functions should be taken into account when discussing the costs and benefits of geoengineering.

Electronic supplementary material The online version of this article (doi:10.1007/s10584-017-1930-3) contains supplementary material, which is available to authorized users.

✉ Akihiko Ito
itoh@nies.go.jp

¹ National Institute for Environmental Studies, 16-2 Onogawa, Tsukuba 305-8506, Japan

² Japan Agency for Marine-Earth Science and Technology, 3173-25 Showa-machi, Yokohama 236-0001, Japan

1 Introduction

SRM, or albedo modification, in which incoming solar radiation is reflected or scattered before reaching to the Earth's surface through the use of technology, is under consideration as a possible cost-efficient option or as an emergency measure to avoid devastating climatic impacts caused by elevated greenhouse gas (GHG) concentrations (Caldeira et al. 2013; Crutzen 2006; Keith and Irvine 2016; Lenton and Vaughan 2009; MacMartin et al. 2014; Robock et al. 2009). Reflection, absorption, and scattering of solar radiation are part of the natural climate system; a conspicuous analogue of SRM is the global cooling that can occur after huge volcanic eruptions (Robock et al. 2013). For example, after the Mt. Pinatubo eruption in June 1991, global mean temperature dropped by about 0.5 K as a result of the injection of approximately 30 Tg of sulphate aerosols into the stratosphere (Soden et al. 2002; Trenberth and Dai 2007). SRM is better quantified than other methods for geoengineering (MacMartin et al. 2016), such that several plausible technologies have been proposed to mimic such phenomenon by controlling these processes, including injection of aerosols into the stratosphere, installation of solar reflector in space, and cloud seeding over the ocean (Keith 2000; Ming et al. 2014). Climate-model studies have assessed the possibility of SRM to prevent anthropogenic GHG-induced temperature rise (Govindasamy and Caldeira 2000; Jones et al. 2016; Lunt et al. 2008; McCusker et al. 2012; Schmidt et al. 2012). As stated below, a model intercomparison project facilitated model-based analyses and impact assessments on geoengineering.

Arguments have been presented related to diverse aspects of geoengineering technologies (e.g. SRM and carbon dioxide removal and sequestration), ranging from their technological feasibility and costs to governance and ethical issues (Bahn et al. 2015; Oldham et al. 2014; Robock et al. 2009). Clearly, geoengineering is not a miracle remedy for global warming; indeed, assessment of its potential benefits and risks has only just started and is gathering attentions. Several studies have investigated the impacts of SRM on physical climate regimes such as El Niño and Southern Oscillation (Gabriel and Robock 2015), tropical cyclone (Moore et al. 2015), quasi-biennial oscillation (Aquila et al. 2014), and climate extremes (Curry et al. 2014). Also many studies have assessed the SRM impacts on hydrological regimes (Ferraro et al. 2014; Kleidon et al. 2015). For example, Bala et al. (2008) conducted simulations using the version 3 of Community Climate Model and found that SRM-caused reduction of incoming solar energy decreases global mean precipitation. From a multi-model simulation study, Tilmes et al. (2013) also found reduction of mean precipitation and frequency of extreme heavy rain. Several studies focused on the effects of SRM on specific phenomena such as sea-level rise (Applegate and Keller 2015; Irvine et al. 2012) and Arctic sea ice and snow cover change (Berdahl et al. 2014; Tilmes et al. 2014).

Climatic and hydrological alterations induced by geoengineering would have influences on aquatic and terrestrial ecosystems (Barrett et al. 2014), including croplands (Parkes et al. 2015; Pongratz et al. 2012; Yang et al. 2016). However, such ramifications are largely unknown because only a small number of studies have conducted such impact assessment. For example, Govindasamy et al. (2002) used the Community Climate Model version 3 including the Integrated Biosphere Simulator to conduct equilibrium simulations for different climate conditions, and assessed the effect of climate stabilization by geoengineering on vegetation changes. Naik et al. (2003) used the Integrated Biosphere Simulator to conduct a series of simulations, including one assuming a lower solar constant (i.e. “geoengineered”), and found negligible impacts on terrestrial productivity. However, remarkably, they found substantial

spatial heterogeneity in the simulated impacts of geoengineering. Eliseev (2012) used a model of the Obukhof Institute of Atmospheric Physics and conducted an RCP8.5-based assessment of SRM deployment, showing that global terrestrial gross productivity would decrease by $17 \text{ Pg C year}^{-1}$ and that there would be a net loss of ecosystem carbon stock of 33 Pg C . In the geoengineering model intercomparison project, Jones et al. (2013) assessed the response of Earth system models in an idealized SRM experiment (G2, +1% CO_2 rise balanced by sulphate aerosol injection and sudden termination) and found that impacts on global terrestrial net primary productivity due to the termination of SRM were inconsistent among models. Muri et al. (2015) assessed the response of tropical forests to SRM deployment by marine sky brightening (G3seasalt experiment) in three Earth system models and found that tropical gross productivity would decrease, partly as a result of salt damage. Kalidindi et al. (2015) used Community Atmosphere Model version 4 to conduct two simplified experiments (sulphate injection and solar constant reduction) and found that SRM deployment would decrease global terrestrial productivity by $\sim 8\%$. Xia et al. (2016) used Community Earth System Model—Community Atmospheric Model 4 to conduct simulations with the RCP6.0 and a transient SRM scenario; they found that SRM deployment increased global terrestrial productivity by $3.8 \pm 1.1 \text{ Pg C year}^{-1}$. Nevertheless, previous studies used only a few models to examine a small number of scenarios, and therefore, they could not adequately consider the range of uncertainty. On the ecological impacts of geoengineering, several narrative reviews have been published (McCormack et al. 2016; Russell et al. 2012) but few systematic evaluations have been conducted using multiple scenarios.

In this study, I conducted a series of simulations with a process-based terrestrial ecosystem model using climate projection scenarios and assessed the impacts of SRM deployment on terrestrial ecosystem functions. Using multiple climate-model projections allows us to evaluate the range of uncertainty caused by differences in climate models and scenarios. Although part of ecosystem responses to SRM has been addressed in previous climate-model studies, adopting the process-based model allows us to resolve broad-scale phenomena into specific factors and underlying mechanisms. I focused on representative ecosystem functions such as productivity, carbon budget, and water budget, which are regulated by biogeochemical and ecophysiological factors. To reveal a further aspect of SRM-induced impacts, I examined the termination effect (Jones et al. 2013; McCusker et al. 2014) of climatic change.

2 Methods and data

2.1 Climate scenarios

This study used climate projection data to drive a terrestrial ecosystem model (described later). For SRM impact experiments, climate projections of Geoengineering Model Intercomparison Project (GeoMIP; Kravitz et al. 2013) were used, and for the reference (without SRM) experiment, data of coupled model intercomparison phase 5 (CMIP5; Taylor et al. 2012) with compatible model configurations were used. For each experiment, outputs of near-surface air temperature, precipitation, and downward shortwave radiation (separated into direct and diffuse components) were used as input of the terrestrial ecosystem model. The climate projection data of 11 climate models were obtained from the Program for Climate Model Diagnosis and Intercomparison (PCMDI) site [URL: <http://www-pcmdi.llnl.gov/>]. For the past period (1850–2005), the output of a historical concentration-driven CMIP5 experiment was

used. For the reference climate projection, outputs of RCP4.5 (Moss et al. 2010) experiments by each climate model were used. In the SRM deployment experiments (mainly by stratospheric aerosol injection), climate model outputs of the G3 and G4 scenarios (Yu et al. 2015) were used for the period from 2020 to 2080, with termination in 2069 and post-termination during 2070–2080. The G3 and G4 scenarios were selected because they assume fairly realistic conditions, whereas the G1 and G2 experiments were conducted assuming idealized conditions for demonstration. See Glienke et al. (2015) for the simulated responses of terrestrial productivity under the G1 scenario, which assumes the abrupt quadrupling of atmospheric CO₂ concentration. In the G3 experiment, sulphate aerosols are injected into the tropical lower stratosphere from 2020 to 2069, such that radiative forcing by the atmospheric greenhouse gas increase is just offset. In the G4 experiment, sulphate aerosols are injected at a constant rate (5 Tg year⁻¹) into the tropical lower stratosphere from 2020 to 2069; thus, negative radiative forcing is assumed to have immediate impacts. In addition to these base scenarios considering stratospheric aerosol injection, experiments with some of the climate models used scenarios considering different technologies (Table 1). In the G3S experiment, a space solar reflector was used instead of sulphate aerosols for SRM. In the G4 cdnc experiment, the liquid cloud droplet concentration of low oceanic clouds was increased by 50% by providing cloud concentration nuclei. In the G3seasalt and G4seasalt experiments, sea salt spray was injected into the marine boundary layer between 30°N and 30°S.

2.2 Description of VISIT model and simulation

A process-based terrestrial ecosystem model, the Vegetation Integrative Simulator for Trace gases (VISIT; Inatomi et al. 2010; Ito 2010), was adopted to simulate the water budget and biogeochemical carbon cycle under changing environments. This model has intermediate complexity in terms of biogeochemistry and ecophysiology, allowing us to conduct multiple simulations for assessing uncertainty and underlying mechanisms. The VISIT model was driven by atmospheric greenhouse gas concentrations, climate parameters, and land-use changes. The land-surface water budget and soil moisture content are simulated by using a simple two-layer hydrological scheme. Runoff discharge is estimated with a bucket model, and evapotranspiration is evaluated with the Penman-Monteith equation, taking account of soil water availability (Ito and Inatomi 2012). The carbon cycle scheme includes C₃ and C₄ plants

Table 1 Summary of GeoMIP climate models and experiments used in this study

Climate models	Experiments
BNU-ESM	RCP4.5, G3, and G4
CanESM2	RCP4.5, G4, and G4cdnc
CCSM4	RCP4.5 and G3S
CSIRO-mk3L-1-2	RCP4.5, G3S, and G4
GISS-EL-R	RCP4.5, G3, and G4
HadGEM2-ES	RCP4.5, G3, G3S, G4, G4cdnc, and G4seasalt
IPSL-CM54-LR	RCP4.5, G3, and G3seasalt (G5)
MIROC-ESM	RCP4.5, G4, and G4cdnc
MIROC-ESM-CHEM	RCP4.5 and G4
MPI-ESM-LR	RCP4.5 and G3
NorESM1-M	RCP4.5 and G4cdnc

and soil organic carbon components, each of which is composed of a few functional compartments (see Ito and Oikawa (2002) for details). Carbon flows in a terrestrial ecosystem are simulated in an ecophysiological manner. Gross primary production (GPP) is estimated for C_3 and C_4 plants, using biome-specific parameters, by analytically integrating single-leaf photosynthesis for the whole canopy. Limitations of atmospheric CO_2 , air humidity via stomatal openings, temperature, and soil moisture are considered. Net ecosystem production (NEP), which represents the CO_2 budget, is obtained as the difference between GPP and ecosystem (plant + microbial) respiration.

Global simulations were conducted at a spatial resolution of $0.5^\circ \times 0.5^\circ$ in latitude and longitude. All the GeoMIP climate projection data were resampled at the simulation resolution and corrected for the historical period by using the observation-based climate data (CRU-TS3.23; Harris et al. 2014). Future climate condition was given by adding anomalies from the average during the baseline period (1970–1999). Photosynthetically active radiation (PAR, 400–700 nm) and its direct and diffuse fractions were estimated at each time step using empirical equations (Supplementary Information). After 300–2000 years of spin-up (until stabilization among the grids was obtained), a historical simulation was conducted for 1901 to 2005. Then simulations for 2006–2019 were forced by the RCP4.5-based projections of the climate models. Finally, the model was forced by the climate projections and RCP4.5-based atmospheric greenhouse gas concentrations during the SRM deployment (2020–2069) and post-termination (2070–2080) periods.

The VISIT model has been tested at site, regional, and global scales, and its performance has been verified through comparisons with many observation data and other models. For example, the present global terrestrial net primary productivity ($61.8 \text{ Pg C year}^{-1}$, average of 2003–2012) is close to meta-analysis results for satellite- and field-based observations (Ito 2011). In this study, I first confirmed that the model behavior was consistent between the VISIT and land-surface schemes implemented in the GeoMIP climate models (Supplementary Fig. S1); the result was convincing for us to conduct in-depth analyses of these functions.

3 Results and discussion

3.1 Climate change in CMIP5 and GeoMIP projections

The CMIP5 and GeoMIP climate projections indicated future temperature rise but at different magnitudes. From the 2000s to the 2060s, the mean land temperature increased by $2.5 \pm 0.6 \text{ K}$ for in the reference scenario ($\delta_{RCP4.5}$), by $1.3 \pm 0.5 \text{ K}$ in the G3 simulations (δ_{G3}), and by $1.7 \pm 0.7 \text{ K}$ (δ_{G4}) in the G4 simulations, respectively (average \pm standard deviation of projections). Here, the difference between $\delta_{RCP4.5}$ and δ_{G3} or δ_{G4} is defined as the SRM-induced impact (Δ): therefore, $\Delta_{G3} = -1.2 \text{ K}$ and $\Delta_{G4} = -0.7 \text{ K}$ (Figs. 1a and 2a; see Fig. S6 for distribution). Future changes in precipitation were also differently simulated in CMIP5 and GeoMIP climate projections. Compared with the reference climate change scenario ($\delta_{RCP4.5}$), precipitation changes were slightly suppressed ($\Delta = -5$ to -20 mm year^{-1}) in the G3 and G4 scenarios because of weakened hydrological cycle (Supplementary Fig. S7). As a result of aerosol injection, PAR was more attenuated ($\Delta \approx -30 \text{ mol photon m}^{-2} \text{ year}^{-1}$) before it reached the land surface (Fig. 1b). It is notable that in many subtropical regions, the direct fraction of PAR decreased whereas the diffuse fraction increased (Supplementary Figs S8 and S9).

As a result of compensation, change in total (i.e. direct and diffuse) PAR was not so large as expected from the decrease in direct component (Supplementary Fig. S10).

3.2 Terrestrial productivity under SRM scenarios

Using the CMIP5 (reference RCP4.5) and GeoMIP climate projections, changes in terrestrial ecosystem functions were simulated by the VISIT model. In the reference experiment, global terrestrial gross primary production (GPP) increased from $122 \pm 2 \text{ Pg C year}^{-1}$ in the 2000s to $146 \pm 6 \text{ Pg C year}^{-1}$ in the 2060s (i.e. $\delta_{\text{RCP4.5}} = 24 \text{ Pg C year}^{-1}$). The GPP amounts simulated in the SRM-based experiments were not significantly different from the reference at global scale ($\Delta = -2.1$ to $+1.6 \text{ Pg C year}^{-1}$;

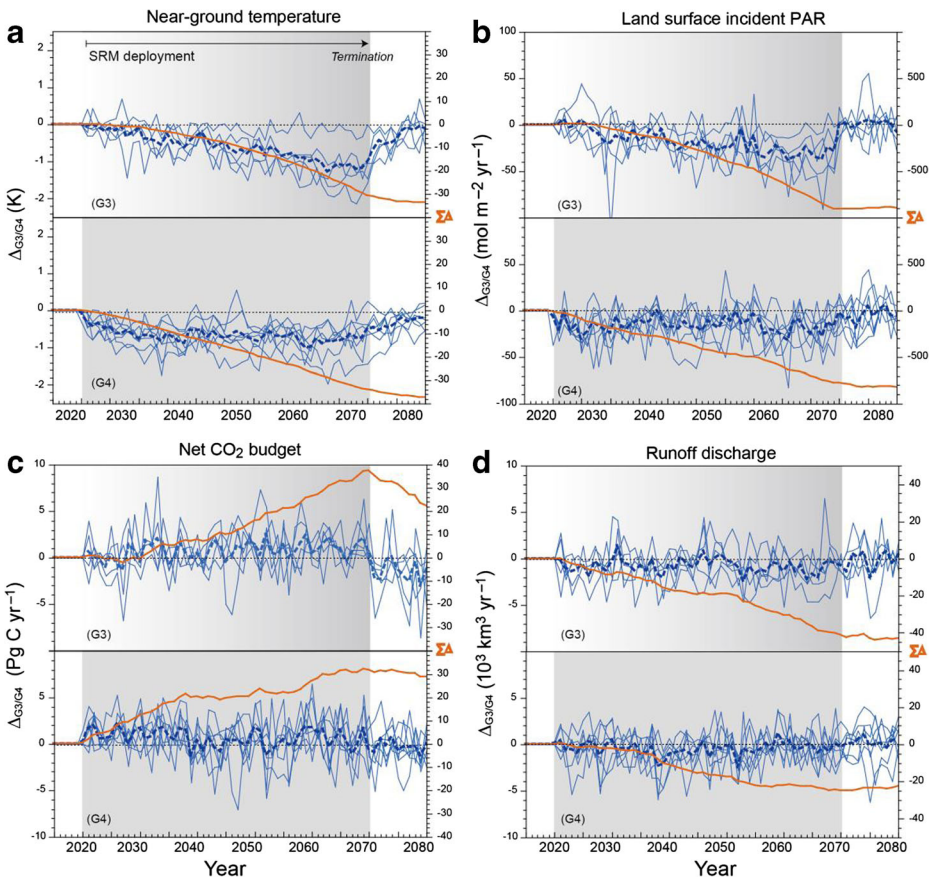


Fig. 1 Simulated trajectories of SRM-induced change (Δ). Differences in **a** the annual mean near-ground temperature change or **b** the land-surface mean annual incident photosynthetically active radiation (PAR) estimated from shortwave radiation by GeoMIP climate models (see the “Methods and data” section) between the reference ($\delta_{\text{RCP4.5}}$) and SRM (δ_{G3} or δ_{G4}) experiments simulated by GeoMIP models during the deployment period (2020–2069). *Thin blue lines* show the results for each climate-model projection, *thick broken blue lines* show the ensemble mean, and *orange lines* show the cumulative difference ($\Sigma\Delta$). Both the RCP4.5-based and SRM simulations assumed the same GHG pathway. Δ for **c**, annual total net ecosystem production (CO₂ budget) or **d**, annual total runoff discharge, simulated by the VISIT model driven by GeoMIP climate projections in an offline manner. See Supplementary Figure S2 for other variables

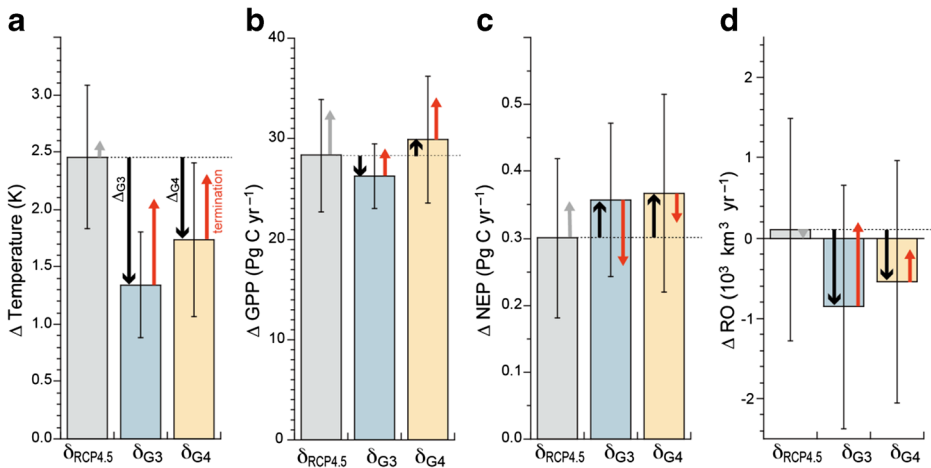


Fig. 2 Changes in terrestrial parameters from the present to the 2060s. **a** Mean annual land temperature simulated by GeoMIP climate models in the reference ($\delta_{RCP4.5}$), G3 (δ_{G3}), and G4 (δ_{G4}) experiments. **b** Annual total gross primary production (GPP), **c** annual total net ecosystem production (NEP), and **d** runoff discharge (RO) in corresponding experiments simulated by VISIT. The difference between $\delta_{RCP4.5}$ and δ_{G3} or δ_{G4} represents the SRM-induced impact (Δ , indicated by *black arrows*). *Red arrows* show the termination effect simulated in the 2070s (shown in *grey* for RCP4.5). See Supplementary Figures S2, S4, and S5 for individual model results

Fig. 2b), but the SRM-induced impact was distributed heterogeneously over the land area (Supplementary Fig. S13), with tropical and subtropical ecosystems showing substantial increases ($\Delta > 1 \text{ Mg C ha}^{-1} \text{ year}^{-1}$).

Several mechanisms could account for the GPP response to SRM. The SRM-induced GPP enhancement in lower latitudes may be attributable to (1) increased PAR absorption by the canopy (APAR) or (2) improved photosynthetic light-use efficiency (LUE = GPP/APAR). Previous studies (Mercado et al. 2009; Xia et al. 2016) showed that an increase of the diffuse light fraction would enhance photosynthetic assimilation, especially in light-limited rainforest ecosystems (Nemani et al. 2003). The process-model approach allowed structural and physiological mechanisms of the GPP enhancement to be separated. APAR increased markedly in subtropical regions (e.g. South Asia and Africa), whereas it increased little in the humid tropics such as Amazonia (Supplementary Fig. S11). In contrast, in humid tropical regions, LUE and GPP were more enhanced in the SRM scenarios, a result that implies that tropical vegetation can convert the solar energy into biomass more efficiently (Supplementary Figs. S12 and S13). It is important that temperature rise in the SRM experiments was substantially ameliorated in the tropics (Supplementary Figure S6), where further warming could exert adverse influences on ecosystems. The retarded warming in lower latitudes was beneficial for productivity due to higher photosynthetic quantum yield and lower respiratory loss. Also, rainforests are in general not water-limited; therefore, the weakened hydrology associated with the G3 and G4 scenarios did not exert an adverse effect on these tropical ecosystems. In contrast, in the subtropics, the retarded warming could enhance vegetation productivity by ameliorating water stress due to lower evaporative demand, allowing vegetation to hold higher leaf area and to absorb more solar radiation (Supplementary Fig. S11). Such GPP responses to SRM in the tropics and subtropics are consistent with the analysis of idealized experimental results by Glienke et al. (2015). In contrast, in the G3- and G4-based experiments, GPP

in temperate to boreal (i.e. temperature-limited) ecosystems did not increase as much as in the reference scenario. In these temperature-limited regions, the smaller temperature rise in SRM-based experiments would restrict the length of growing period and then photosynthetic productivity in comparison with the reference case.

3.3 Terrestrial carbon and water budgets under SRM scenarios

The retarded temperature rise in the SRM-based climate projections, although warming was not completely prevented, suppressed the increase of respiratory CO₂ emissions in the VISIT simulations ($\Delta_{G3} = -1.5 \pm 2.3 \text{ Pg C year}^{-1}$ and $\Delta_{G4} = -0.2 \pm 1.8 \text{ Pg C year}^{-1}$ in the 2060s). Consequently, the cumulative additional net carbon sequestration by the terrestrial biosphere was 34 Pg C (95% confidence interval, -6 to 74 Pg C) during 2020–2069 (Fig. 1c). The G4-based experiments showed higher net ecosystem production (NEP) during the early decades of the SRM deployment than the G3-based experiment, as expected from the aerosol injection pattern, but the G3-based experiments caught up after ca. 2060. SRM-induced carbon uptake was found mainly in lower latitudes (Fig. 3a; see Supplementary Fig. S14 for the G4-based result), where substantial GPP enhancement occurred.

The weakened hydrological cycle (Bala et al. 2008; Tilmes et al. 2013) and altered vegetation activity caused by SRM deployment also affected the terrestrial water budget. Runoff discharge (RO) from terrestrial ecosystems, which relates to the potential water-resource supply, was suppressed in the SRM-based experiments of the VISIT model ($\Delta = -0.65$ to $-0.96 \times 1000 \text{ km}^3 \text{ year}^{-1}$; Fig. 1d; see Supplementary Fig. S15 for the G4-based result). The RO suppression occurred mainly in the humid tropics, where the climate models simulated decreased rainfall (Supplementary Fig. S7). Therefore, the fraction of RO relative to precipitation was not substantially affected in these regions (Supplementary Fig. S16). It is noteworthy that in certain areas such as the Mediterranean region, decreases of precipitation and runoff in the reference scenario were slightly ameliorated in the SRM results.

3.4 Termination impacts

The termination effect is a serious issue of geoengineering, but only a few studies have assessed the impacts of termination on land systems (Jones et al. 2013; Matthews and Caldeira 2007). In the GeoMIP climate projections, after sudden termination of the SRM deployment in 2069, mean land temperature rose rapidly at rates of 0.6 to 0.8 K per decade (Figs. 1a and 2a), and these temperature increases were accompanied by a clear increase of incident PAR. Terrestrial ecosystems, especially in the G3-based experiments, released extra carbon to the atmosphere ($\Delta_{G3} = -1.25 \pm 1.0 \text{ Pg C year}^{-1}$ in the 2070s) mainly as a result of enhanced ecosystem respiration by the rapid warming. A termination effect was also evident in RO simulated by the terrestrial model, which promptly returned amounts close to the reference value (Fig. 1d).

3.5 Difference among SRM technologies

Furthermore, I examined differences in Δ between the sulphate aerosol SRM technology and other technologies for which climate projections were available (cf. Table 1). When a solar reflector in space was used to reduce solar radiation (GeoMIP experiment G3S), the GPP (VISIT simulation) enhancement at lower latitudes caused by retarded temperature

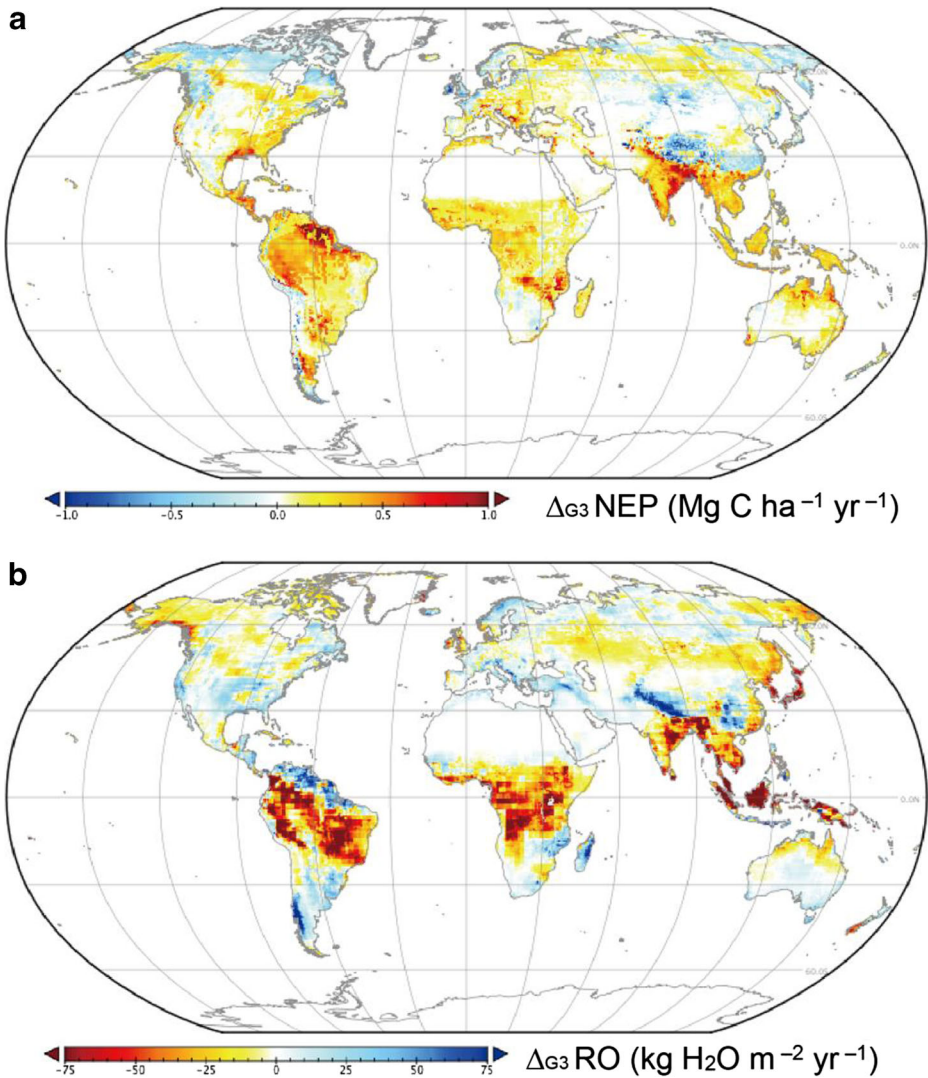


Fig. 3 Simulated distribution of SRM-induced changes (Δ). **a** Annual net ecosystem production (NEP: CO_2 budget, positive for net land sink) and **b** annual runoff discharge (RO, positive for increase) for the G3 result in the 2060s. See Supplementary Figs S14 and S15 for the results of the G4 experiments

rise and increased diffuse radiation largely remained. In addition, GPP in temperate and boreal ecosystems was more suppressed than it was in the G3-based experiments because of the reduced solar radiation at higher latitudes. When cloud droplet number concentration increment (G4cdnc; i.e. cloud seeding) or sea salt spray (G3seasalt and G4seasalt) technologies were adopted, reductions in solar radiation occurred chiefly over ocean areas and SRM-induced impacts on terrestrial functions were substantially ameliorated. These results imply that it is possible to mitigate SRM-induced impacts by selecting appropriate technologies.

4 Concluding remarks

This study used multiple climate projection experiments, as many as available, in an evaluation of SRM-induced impacts on land systems. While previous studies using single models have provided inconsistent results (e.g. positive or negative impacts), this study compared multiple experimental results and examined consistency. Furthermore, this study explored the mechanisms underlying the effects of SRM deployment through the use of the process-based VISIT model.

There remain, however, several limitations to the present approach. The present terrestrial models may need improvement to capture temporal variability in ecosystem functions with higher credibility. Although the performance was largely comparable between the VISIT and other models (Supplementary Fig. S1), there still remain large estimation uncertainties as demonstrated by impact-model intercomparison studies (Friend et al. 2014). For example, it is difficult for many terrestrial models to accurately simulate the extra carbon uptake that occurred after the Mt. Pinatubo eruption (Le Quéré et al. 2016). After the huge eruption, increase in atmospheric CO₂ level was noticeably retarded, presumably as a result of the increased photosynthetic uptake, due to diffused solar radiation, and the decreased respiratory release of CO₂ due to surface cooling (Gu et al. 2003). The present models might not be possible to capture such mechanisms in a quantitative manner. In addition, in this study, I used only a few simplified SRM scenarios of the GeoMIP; these scenarios should be refined further by including socioeconomic and strategic factors (Keith and MacMartin 2015; Kravitz et al. 2016). To achieve a more reliable impact assessment, we need to refine models by using observational data for validation and development and to conduct more interdisciplinary studies.

Nevertheless, the results presented here have implications for climate and risk managements (see Fig. 4). First, climate warming and its impacts were not completely prevented in either SRM scenario, the implication being that concurrent measures such as reducing GHG emissions would be still required. Considering the historical warming since the preindustrial era, temperature rise at the middle of this century is likely to exceed the level adopted in the Paris Agreement. It is noteworthy, however, that SRM by aerosol injection might induce additional carbon sequestration ($\sim 1 \text{ Pg C year}^{-1}$ equivalent to approximately +20% of the no-geoengineering case) in terrestrial ecosystems. The cumulative carbon sequestration during the SRM deployment period is roughly equivalent to a drawdown of atmospheric CO₂ by about 6.4 ppmv (assuming airborne fraction of 0.4; Canadell et al. 2007). Second,

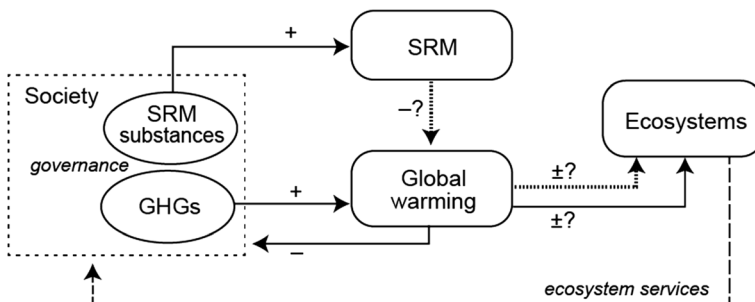


Fig. 4 Impacts of SRM deployment on land systems. Schematic diagram of the impacts of SRM deployment on natural and human systems

the SRM-induced impacts would be heterogeneously distributed among regions and impact sectors (e.g. biomes and hydrological system). The unequal distribution of the induced impacts should be taken into account when discussing the governance of geoengineering. Third, termination effects on land systems, such as the rapid release of the extra carbon, are highly likely after decades-long aerosol injection. The various costs and risks of SRM for all stakeholders should be carefully discussed using an interdisciplinary approach (Cusack et al. 2014; Hegerl and Solomon 2009), although choosing an optimal SRM technology might at least partly mitigate SRM-induced risks.

Acknowledgements This study was conducted as a part of Integrated Climate Assessment—Risks, Uncertainties and Society (ICA-RUS), funded by the Environmental Research Fund of the Ministry of Environment, Japan, and it was also supported in part by a KAKENHI grant (no. 26281014) from the Japan Society for the Promotion of Science. The CMIP5 and GeoMIP model outputs were obtained from the Program for Climate Model Diagnosis and Intercomparison, Lawrence Livermore National Laboratory, a node of the Earth System Grid Federation.

References

- Applegate PJ, Keller K (2015) How effective is albedo modification (solar radiation management geoengineering) in preventing sea-level rise from Greenland Ice Sheet? *Env Res Lett* 10:084018. doi:10.1088/1748-9326/10/10/088/084018
- Aquila V, Garfinkel CI, Newman PA, Oman LD, Waugh DW (2014) Modifications of the quasi-biennial oscillation by a geoengineering perturbation of the stratospheric aerosol layer. *Geophys Res Lett* 41:1738–1744. doi:10.1002/2013GL058818
- Bahn O, Chesney M, Gheysens J, Knutti R, Pana AC (2015) Is there room for geoengineering in the optimal climate policy mix? *Env Sci Policy* 48:67–76
- Bala G, Duffy PB, Taylor KE (2008) Impact of geoengineering schemes on the global hydrological cycle. *Proc Nat Acad Sci USA* 105:7664–7669
- Barrett S, Lenton TM, Millner A, Tavoni A, Carpenter S, Anderies JM, Chapin FSI, Crépin A-S, Daily G, Ehrlich P, Folke C, Galaz V, Hughes T, Kautsky N, Lambin EF, Naylor R, Nyborg K, Polasky S, Scheffer M, Wilen J, Xepapadeas A, de Zeeuw A (2014) Climate engineering reconsidered. *Nat Clim Change* 4:527–529
- Berdahl M, Robock A, Ji D, Moore JC, Jones A, Kravitz B, Watanabe S (2014) Arctic cryosphere response in the Geoengineering Model Intercomparison Project G3 and G4 scenarios. *J Geophys Res* 119:1308–1321
- Caldeira K, Bala G, Cao L (2013) The science of geoengineering. *Ann Rev Earth Planet Sci* 41:231–256
- Canadell JG, Le Quére C, Raupach MR, Field CB, Buitenhuis ET, Ciais P, Conway TJ, Gillett NP, Marland G (2007) Contributions to accelerating atmospheric CO₂ growth from economic activity, carbon intensity, and efficiency of natural sinks. *Proc Nat Acad Sci USA* 104:18866–18870
- Crutzen PJ (2006) Albedo enhancement by stratospheric sulfur injections: a contribution to resolve a policy dilemma? *Clim Change* 77:211–219
- Curry CL, Sillmann J, Bronaugh D, Alterskjaer K, Cole JN, Ji D, Kravitz B, Kristjánsson JE, Moore JC, Muri H, Niemeier U, Robock A, Tilman S, Yang S (2014) A multimodel examination of climate extremes in an idealized geoengineering experiment. *J Geophys Res* 119:3900–3923
- Cusack DF, Axsen J, Shwom R, Hartzell-Nichols L, White S, Mackey KRM (2014) An interdisciplinary assessment of climate engineering strategies. *Front Ecol Env* 12:280–287
- Eliseev AV (2012) Climate change mitigation via sulfate injection to the stratosphere: impact on the global carbon cycle and terrestrial biosphere. *Atm Ocean Opt* 25:405–413
- Ferraro AJ, Highwood EJ, Charlton-Perez AJ (2014) Weakened tropical circulation and reduced precipitation in response to geoengineering. *Env Res Lett* 9:014001. doi:10.1088/1748-9326/9/1/014001
- Friend AD, Lucht W, Rademacher TT, Keribin RM, Betts R, Cadule P, Ciais P, Clark DB, Dankers R, Falloon P, Ito A, Kahana R, Kleidon A, Lomas MR, Nishina K, Ostberg S, Pavlick R, Peylin P, Schaphoff S, Vuichard N, Warszawski L, Wiltshire A, Woodward FI (2014) Carbon residence time dominates uncertainty in terrestrial vegetation responses to future climate and atmospheric CO₂. *Proc Nat Acad Sci USA* 111:3280–3285
- Gabriel CJ, Robock A (2015) Stratospheric geoengineering impacts on El Niño/Southern Oscillation. *Atm Chem Phys* 15:11949–11966
- Glienke S, Irvine PJ, Lawrence MG (2015) The impact of geoengineering on vegetation in experiment G1 to the GeoMIP. *J Geophys Res Atm* 120:10196–10213

- Govindasamy B, Caldeira K (2000) Geoengineering Earth's radiation balance to mitigate CO₂-induced climate change. *Geophys Res Lett* 27:2141–2144
- Govindasamy B, Thompson S, Duffy PB, Caldeira K, Delire C (2002) Impact of geoengineering schemes on the terrestrial biosphere. *Geophys Res Lett* 29:2061. doi:10.1029/2002GL015911
- Gu L, Baldocchi D, Wofsy SC, Munger JW, Michalsky JJ, Urbanski S, Boden TA (2003) Response of a deciduous forest to the Mount Pinatubo eruption: enhanced photosynthesis. *Science* 299:2035–2038
- Harris I, Jones PD, Osborn TJ, Lister DH (2014) Updated high-resolution grids of monthly climatic observations—the CRU TS3.10 dataset. *Int J Climatol* 34:623–642
- Hegerl GC, Solomon S (2009) Risks of climate engineering. *Science* 325:955–956
- Inatomi M, Ito A, Ishijima K, Murayama S (2010) Greenhouse gas budget of a cool temperate deciduous broadleaved forest in Japan estimated using a process-based model. *Ecosystems* 13:472–483
- Irvine PJ, Sriver RL, Keller K (2012) Tension between reducing sea-level rise and global warming through solar-radiation management. *Nat Clim Change* 2:97–100
- Ito A (2010) Changing ecophysiological processes and carbon budget in East Asian ecosystems under near-future changes in climate: implications for long-term monitoring from a process-based model. *J Plant Res* 123:577–588
- Ito A (2011) A historical meta-analysis of global terrestrial net primary productivity: are estimates converging? *Global Change Biol* 17:3161–3175
- Ito A, Inatomi M (2012) Water-use efficiency of the terrestrial biosphere: a model analysis on interactions between the global carbon and water cycles. *J Hydromet* 13:681–694
- Ito A, Oikawa T (2002) A simulation model of the carbon cycle in land ecosystems (Sim-CYCLE): a description based on dry-matter production theory and plot-scale validation. *Ecol Model* 151:147–179
- Jones A, Haywood JM, Alterskjær K, Boucher O, Cole JNS, Curry CL, Irvine PJ, Ji D, Kravitz B, Kristjánsson JE, Moore JC, Niemeier U, Robock A, Schmidt H, Singh B, Tilmes S, Watanabe S, Yoon J-H (2013) The impact of abrupt suspension of solar radiation management (termination effect) in experiment G2 of the Geoengineering Model Intercomparison Project (GeoMIP). *J Geophys Res* 118:9743–9752
- Jones AC, Haywood JM, Jones A (2016) Climatic impacts of stratospheric geoengineering with sulfate, black carbon and titania injection. *Atm Chem Phys* 16:2843–2862
- Kalidindi S, Bala G, Modak A, Caldeira K (2015) Modeling of solar radiation management: a comparison of simulations using reduced solar constant and stratospheric sulphate aerosols. *Clim Dyn* 44:2909–2925
- Keith DW (2000) Geoengineering the climate: history and prospect. *Ann Rev Energy Environ* 25:245–284
- Keith DW, Irvine PJ (2016) Solar geoengineering could substantially reduce climate risks—a research hypothesis for the next decade. *Earth's Future* 4:549–559
- Keith DW, MacMartin DG (2015) A temporary, moderate and responsive scenario for solar geoengineering. *Nat Clim Change* 5:201–206
- Kleidon A, Kravitz B, Renner M (2015) The hydrological sensitivity to global warming and solar geoengineering derived from thermodynamic constraints. *Geophys Res Lett* 42:138–144
- Kravitz B, Caldeira K, Boucher O, Robock A, Rasch PJ, Alterskjær K, Irvine PJ, Ji D, Jones A, Kristjánsson JE, Lunt DJ, Moore JC, Niemeier U, Schmidt H, Schulz M, Singh B, Tilmes S, Watanabe S, Yang S, Yoon J-H (2013) Climate model response from the Geoengineering Model Intercomparison Project (GeoMIP). *J Geophys Res* 118:8320–8332
- Kravitz B, MacMartin DG, Wang H, Rasch PJ (2016) Geoengineering as a design problem. *Earth Sys Dyn* 7:469–497
- Le Quéré C, Andrew RM, Canadell JG, Sitch S, Korsbakken JJ, Peters GP, Manning AC, Boden TA, Tans PP, Houghton RA, Keeling RF, Alin S, Andrews OD, Anthoni P, Barbero L, Bopp L, Chevallier F, Chini LP, Ciais P, Currie K, Delire C, Doney SC, Friedlingstein P, Gkritzalis T, Harris I, Hauck J, Haverd V, Hoppema M, Klein Goldewijk K, Jain AK, Kato E, Körtzinger A, Landschützer P, Lefèvre N, Lenton A, Lienert S, Lombardozzi D, Melton JR, Metzl N, Millero F, Monteiro PMS, Munro DR, Nabel JEMS, Nakaoka S, O'Brien K, Olsen A, Omar AM, Ono T, Pierrot D, Poulter B, Rödenbeck C, Salisbury J, Schuster U, Schwinger J, Séférian R, Skjelvan I, Stocker BD, Sutton AJ, Takahashi T, Tian H, Tilbrook B, van der Laan-Luijkx IT, van der Werf GR, Viovy N, Walker AP, Wiltshire AJ, Zaehle S (2016) Global carbon budget 2016. *Earth Sys Sci Data* 8:605–649
- Lenton TM, Vaughan NE (2009) The radiative forcing potential of different climate geoengineering options. *Atm Chem Phys* 9:5539–5561
- Lunt DJ, Ridgwell A, Valdes PJ, Seale A (2008) “Sunshade world”: a fully coupled GCM evaluation of the climatic impacts of geoengineering. *Geophys Res Lett* 35:L12710. doi:10.1029/2008GL033674
- MacMartin DG, Caldeira K, Keith DW (2014) Solar geoengineering to limit the rate of temperature change. *Phil Trans Roy Soc A* 372:20140134. doi:10.1098/rsta.2014.0134
- MacMartin DG, Kravitz B, Long JCS, Rasch PJ (2016) Geoengineering with stratospheric aerosols: what do we not know after a decade of research? *Earth's Future* 4:543–548

- Matthews HD, Caldeira K (2007) Transient climate–carbon simulations of planetary geoengineering. *Proc Nat Acad Sci USA* 104:9949–9954
- McCormack CG, Born W, Irvine PJ, Achterberg EP, Amano T, Ardron J, Foster PN, Gattuso J-P, Hawkins SJ, Hendy E, Kissling WD, Lluch-Cota SE, Murphy EJ, Ostle N, Owens NJP, Perry RI, Pörtner HO, Scholes RJ, Schuur FM, Schweiger O, Settele J, Smith RK, Smith S, Thompson J, Tittensor DP, van Kleunen M, Vivian C, Vohland K, Warren R, Watkinson AR, Widdicombe S, Williamson P, Woods E, Blackstock JJ, Sutherland WJ (2016) Key impacts of climate engineering on biodiversity and ecosystems, with priorities for future research. *J Integr Env Sci* 13:103–128
- McCusker KE, Armour KC, Bitz CM, Battisti DS (2014) Rapid and extensive warming following cessation of solar radiation management. *Env Res Lett* 9:024005. doi:10.1088/1748-9326/1089/1082/024005
- McCusker KE, Battisti DS, Bitz CM (2012) The climate response to stratospheric sulfate injections and implications for addressing climate emergencies. *J Clim* 25:3096–3116
- Mercado LM, Bellouin N, Sitch S, Boucher O, Huntingford C, Wild M, Cox PM (2009) Impact of changes in diffuse radiation on the global land carbon sink. *Nature* 458:1014–1017
- Ming T, de Richter R, Liu W, Caillol S (2014) Fighting global warming by climate engineering: is the earth radiation management and the solar radiation management any options for fighting climate change? *Renew Sustain Energy Rev* 31:792–834
- Moore JC, Grinstead A, Guo X, Yu X, Jevrejeva S, Rinke A, Cui X, Kravitz B, Lenton A, Watanabe S, Ji D (2015) Atlantic hurricane surge response to geoengineering. *Proc Nat Acad Sci USA* 112:13794–13799
- Moss RH, Edmonds JA, Hibbard KA, Manning MR, Rose SK, van Vuuren DP, Carter TR, Emori S, Kainuma M, Kram T, Meehl GA, Mitchell JFB, Nakicenovic N, Riahi K, Smith SJ, Stouffer RJ, Thomson AM, Weyant JP, Wilbanks TJ (2010) The next generation of scenarios for climate change research and assessment. *Nature* 463:747–756
- Muri H, Niemeier U, Kristjánsson JE (2015) Tropical rainforest response to marine sky brightening climate engineering. *Geophys Res Lett* 42:2951–2960
- Naik V, Wuebbles DJ, Delucia EH, Foley JA (2003) Influence of geoengineered climate on the terrestrial biosphere. *Env Manag* 32:373–381
- Nemani RR, Keeling CD, Hashimoto H, Jolly WM, Piper SC, Tucker CJ, Myrneni RB, Running SW (2003) Climate-driven increases in global terrestrial net primary production from 1982 to 1999. *Science* 300:1560–1563
- Oldham P, Szerszynski B, Stilgoe J, Brown C, Eacott B, Yuille A (2014) Mapping the landscape of climate engineering. *Phil Trans Roy Soc A* 372:20140065. doi:10.1098/rsta.2014.0065
- Parkes B, Challinor A, Nicklin K (2015) Crop failure rates in a geoengineered climate: impact of climate change and marine cloud brightening. *Env Res Lett* 10:084003. doi:10.1088/1748-9326/1010/1088/084003
- Pongratz J, Lobell DB, Cao L, Caldeira K (2012) Crop yields in a geoengineered climate. *Nat Clim Change* 2:101–105
- Robock A, MacMartin DG, Duren R, Christensen MW (2013) Studying geoengineering with natural and anthropogenic analogs. *Clim Change* 121:445–458
- Robock A, Marquardt A, Kravitz B, Stenchikov G (2009) Benefits, risks, and costs of stratospheric geoengineering. *Geophys Res Lett* 36:L19703. doi:10.1029/2009GL039209
- Russell LM, Rasch PJ, Mace GM, Jackson RB, Shepherd J, Liss P, Leinen M, Schimel D, Vaughan NE, Janetos AC, Boyd PW, Norby RJ, Caldeira K, Merikanto J, Artaxo P, Melillo J, Morgan MG (2012) Ecosystem impacts of geoengineering: a review for developing a science plan. *Ambio* 41:350–369
- Schmidt H, Alterskjær K, Karam DB, Boucher O, Jones A, Kristjánsson JE, Niemeier U, Schulz M, Aaheim A, Benduhn F, Lawrence M, Timmreck C (2012) Solar irradiance reduction to counteract radiative forcing from a quadrupling of CO₂: climate responses simulated by four earth system models. *Earth Syst Dyn* 3:63–78
- Soden BJ, Wetherald RT, Stenchikov GL, Robock A (2002) Global cooling after the eruption of Mount Pinatubo: a test of climate feedback by water vapor. *Science* 296:727–730
- Taylor KE, Stouffer RJ, Meehl GA (2012) An overview of CMIP5 and the experiment design. *Bull Am Meteorol Soc* 93:485–498
- Tilmes S, Fasullo J, Lamarque J-F, Marsh DR, Mills M, Alterskjær K, Muri H, Kristjánsson JE, Boucher O, Schulz M, Cole JNS, Curry CL, Jones A, Haywood J, Irvine PJ, Ji D, Moore JC, Karam DB, Kravitz B, Rasch PJ, Singh B, Yoon J-H, Niemeier U, Schmidt H, Robock A, Yang S, Watanabe S (2013) The hydrological impact of geoengineering in the Geoengineering Model Intercomparison Project (GeoMIP). *J Geophys Res* 118:11036–11058
- Tilmes S, Jahn A, Kay JE, Holland M, Lamarque J-F (2014) Can regional climate engineering save the summer Arctic Sea Ice? *Geophys Res Lett* 41:880–885
- Trenberth KE, Dai A (2007) Effects of Mount Pinatubo volcanic eruption on the hydrological cycle as an analog of geoengineering. *Geophys Res Lett* 34:L15702. doi:10.1029/2007GL030524
- Xia L, Robock A, Tilmes S, Neely RRI (2016) Stratospheric sulfate geoengineering could enhance the terrestrial photosynthesis rate. *Atm Chem Phys* 16:1479–1489

- Yang H, Dobbie S, Ramirez-Villegas J, Feng K, Challinor AJ, Chen B, Gao Y, Lee L, Yin Y, Sun L, Watson J, Koehler A-K, Fan T, Ghosh S (2016) Potential negative consequences of geoengineering on crop production: a study of Indian groundnut. *Geophys Res Lett* 43:11786–11795
- Yu X, Moore JC, Cui X, Rinke A, Ji D, Kravitz B, Yoon J-H (2015) Impacts, effectiveness and regional inequalities of the GeoMIP G1 to G4 solar radiation management scenarios. *Global Planet Change* 129:10–22